



University of Iowa Honors Theses


University of Iowa Honors Program

Spring 2018

EQE Measurements in Mid-Infrared Superlattice Structures

Andrew Muellerleile

Follow this and additional works at: http://ir.uiowa.edu/honors_theses

 Part of the [Condensed Matter Physics Commons](#), and the [Optics Commons](#)

Copyright © 2018 Andrew Muellerleile

Hosted by [Iowa Research Online](#). For more information please contact: lib-ir@uiowa.edu.

EQE MEASUREMENTS IN MID-INFRARED SUPERLATTICE STRUCTURES

by

Andrew Muellerleile

A thesis submitted in partial fulfillment of the requirements
for graduation with Honors in the Physics

John Prineas
Thesis Mentor

Spring 2018

All requirements for graduation with Honors in the
Physics have been completed.

Vincent Rogers
Physics Honors Advisor

EQE Measurements in Mid-Infrared Superlattice Structures
Andrew Muellerleile
Spring 2018
Advised by John P. Prineas PhD

Abstract:

LEDs, or light emitting diodes, are perhaps one of the most visible semiconductor devices in everyday life. They appear as the power indicators on household devices, light up the hallway in the form of LED lightbulbs, and even show up as the pixels in OLED, or organic light emitting diode, television sets. From these applications, it's easy to see that LEDs operating in the visible portion of the electromagnetic spectrum, or between 400 and 700nm, are commonplace. Nearly as commonplace are LEDs operating in the NIR, near infrared, from the red edge of the visible at around 700 nm to around 1 micron. These are present in the remote control of your TV, but perhaps more importantly as the diode lasers used in telecommunications for sending data over fiber optic cables. Because of their numerous applications, research by industry has made visible and NIR LEDs increasingly cheap, efficient and therefore abundant. Comparatively less common, and therefore less developed, are devices for emitting light in the frequency range between 3 and 5 microns, known as the mid-infrared or thermal infrared. This is unfortunate, because such devices have thermal imaging applications in the military and numerous potential applications in gas sensing. LEDs in this region suffer numerous problems, primarily in wall-plug efficiency, which is frequently below 1%, which limits their potential applications. These problems are the impetus for EIRE, which stands for Efficient InfraRed Emitters. EIRE seeks to solve the efficiency problems through the use of III-V superlattices as an emission material. My part in this project was to measure the External Quantum Efficiency (EQE) of the superlattice structures we grew, which is key in developing more efficient devices.

Theory:

A superlattice is a semiconductor heterostructure composed of two or more semiconducting materials deposited in very thin layers so as to engineer the properties of the bulk device as desired. The underlying mechanism is that the alternating semiconductor layers can be made thinner than the wavelength of the charge carriers in the individual semiconductors. This means that the charge carriers are not fully confined in a single layer, and therefore the band structure of the material depends on the

thickness and spacing of the individual materials. An alternate interpretation is that a superlattice is essentially a series of coupled quantum wells with boundary layers thin enough that the eigenstates become delocalized over the entire superlattice region, meaning that they form bands with properties determined by the structure of the layered semiconductors. This is in contrast to larger heterostructures where the band structure of the bulk device is assumed to be identical to that of a bulk semiconductor in each region. The ability to fine-tune the bulk electrical properties of a device based on fine structural details is extremely important with the advent of epitaxial growth techniques which can deposit very thin layers with a controlled composition, such as molecular beam epitaxy. For example, for a conventional LED to emit radiation at 3 microns requires a material with a band gap around 0.4 eV. An alloy of III-V materials such as GaSb and InSb would allow the creation of a band gap in this range, but the structure of low-lying valence bands could not be changed. However, by tuning the layer thickness in the superlattice it is possible to change the position of these bands, which allows a reduction in Auger recombination. This ability to control the band structure of a material is important for the EIRE project, as it allows a reduction in recombination modes which decrease efficiency.

The efficiency of light-emitting semiconductor devices depends on the way in which energy added to the device, in the form of electric current or absorbed photons, is changed into light or lost as heat. This in turn depends on the recombination methods possible for the electrons and holes produced in the device. For LEDs there are three major recombination modes: Shockley–Read–Hall recombination, Auger recombination, and radiative recombination. Radiative recombination is the most desired, as this

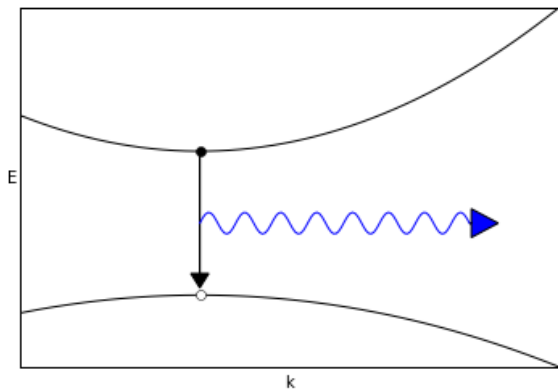


Fig 1. Radiative Recombination - an electron and hole recombine producing a photon

mode actually produces the light in the LED. It is also has the simplest mechanism. In a direct gap semiconductor, like those used in our devices, an electron excited to the conduction band recombines with a hole in the valence band at the same k-value which produces a photon. The energy of the photon produced corresponds exactly to the energy difference of the electron and hole states, meaning that if this were the only method of recombination in a device it would

have perfect quantum efficiency. Unfortunately this isn't possible in practice, as non-radiative recombination modes also contribute. Shockley–Read–Hall recombination is where deep impurity states trap charge carriers which then recombine, but instead of producing a photon the energy is dissipated as lattice vibrations (phonons) in the crystal. This changes the energy added to the device into heat, and therefore is a source of inefficiency. Auger recombination is also a source of loss in devices, but unlike SRH recombination which involves only a single charge carrier and radiative recombination which involves two charge carriers, Auger recombination involves three charge carriers. Because of this it tends to dominate at very high carrier concentrations. Specifically, Auger recombination is a process where an electron and hole recombine and transfer the energy to a third charge carrier in a higher or lower band. These charge carriers do not contribute to the light emitted by the device and instead tend to disperse energy as heat in secondary recombination events, which means that Auger recombination is a source of loss in LEDs.

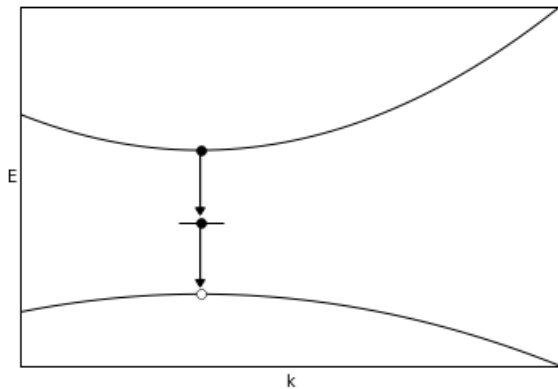


Fig 2. Trap-assisted (SRH) recombination - an electron becomes trapped in a deep acceptor level, then recombines with a hole

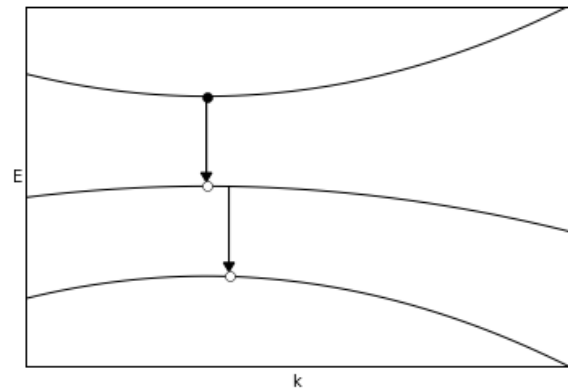


Fig 3. Auger recombination - an electron and hole excite a second hole to a lower band

Non-radiative recombination will act as a source of loss in any physical device, but luckily both SRH and Auger recombination can be minimized by clever manipulation of the band structure. In theory SRH is easy to minimize by reducing the concentration of trap levels in a semiconductor. However, in III-V materials there will always be a proportion of native defects with even the purest raw materials and growth methods. These will inevitably contribute trap levels which can participate in SRH recombination.

Fortunately, for a given crystal structure the trap levels due to a specific impurity always have the same energy. This means that the band energies of the device can be adjusted so that common defect states are not in the middle of the band-gap, which can greatly reduce SRH recombination. Auger recombination can also be reduced by changing the band structure of a material, as there must be lower bands within a band gap energy for the excited holes to be excited into. This is where superlattice structures shine, as by adjusting the layer spacing it is possible to change the position of low-lying bands in exactly this way. The figure below shows an un-optimized superlattice on the left and an optimized superlattice on the right:

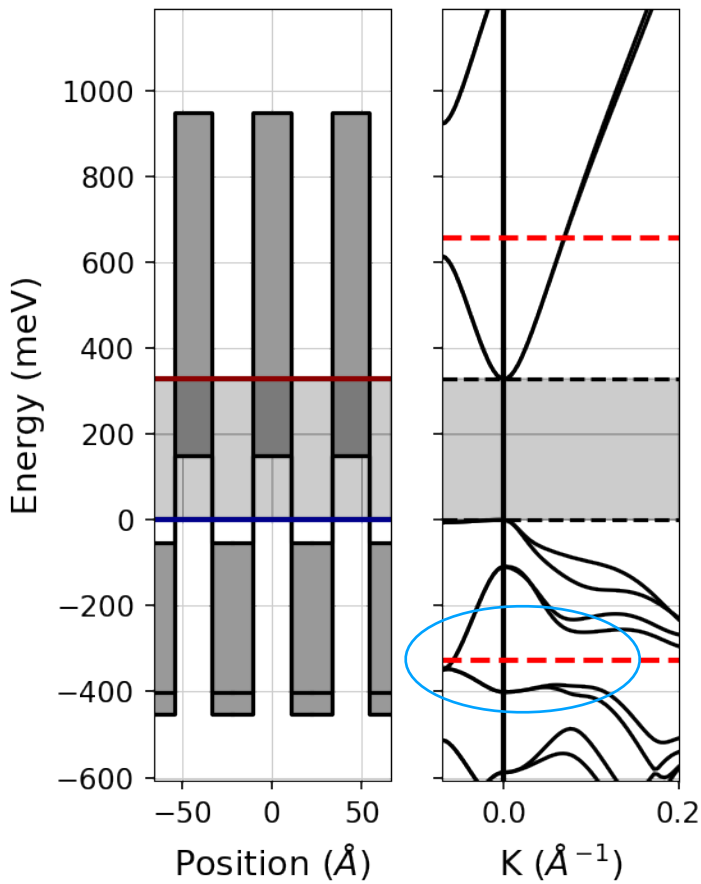


Figure 4. Unoptimized Superlattice

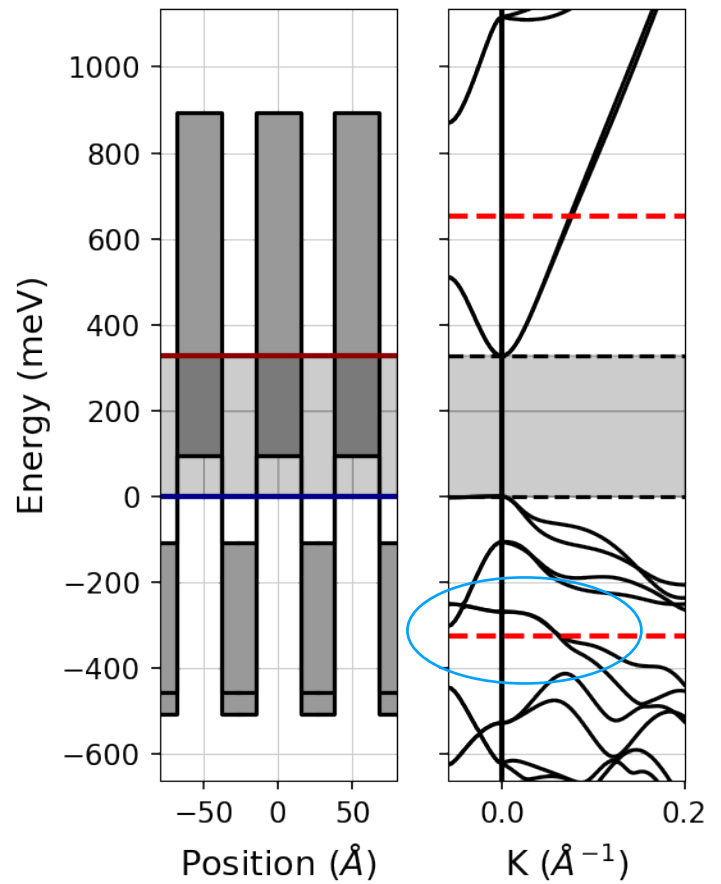


Figure 5. Optimized Superlattice

In the unoptimized superlattice there are states in lower-lying bands at one band gap energy (shown by the red dotted line) of the valence band, which means that holes can be excited to it via Auger recombination.

However, in the figure on the right these states are moved up in energy, meaning that Auger recombination cannot excite holes into these states, which reduces its likelihood of occurring. Although in theory it is easy to grow structures with improved efficiency, it is important to be able to characterize the recombination modes actually occurring in devices we've created. A useful model used to do this is ABC theory, which says that the carrier recombination rate per unit volume, R , in a semiconductor is related to carrier density n by:

$$\text{Equation 1: } R = A*n + B*n^2 + C*n^3$$

where A , B and C are constants determining the Shockley–Read–Hall, radiative, and Auger recombination rates respectively. Dividing by n gives the radiative rate per carrier:

$$\text{Equation 2: } \frac{R}{n} = A + B*n + C*n^2$$

Because of this relationship between recombination rate and carrier density, it is possible to measure the recombination rate at various carrier densities and create a plot like the following:

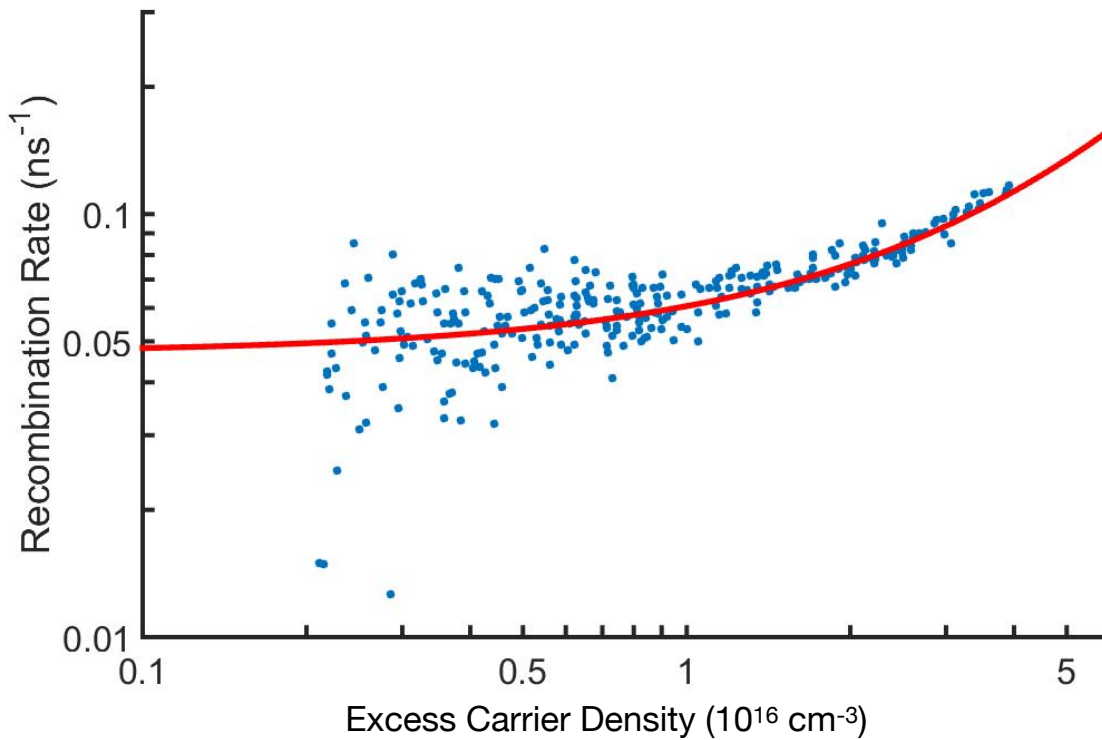


Figure 6. Plot of carrier recombination rate vs. carrier density

Performing a quadratic fit can then give the A, B and C coefficients which quantifies the prevalence of different recombination modes. However, this type of measurement is sensitive to instrumental and systematic uncertainties because of the fitting process. It is also time-consuming, as measuring the total recombination rate requires an experimental setup which can measure carrier density on nanosecond time scales. However, it is possible to perform a simpler measurement which gives much of the same information. The most important information to know about a light-emitting device is its efficiency, which is a ratio of the photons generated to the electron-hole pairs input to the system. This quantity is the IQE, or internal quantum efficiency. In the context of ABC theory, the internal quantum efficiency is given by:

Equation 3:

$$IQE = \frac{B * n^2}{R} = \frac{B * n}{A + B * n + C * n^2}$$

However, this can also be measured in a direct measurement by using the EQE, or external quantum efficiency. This is related to IQE by the extraction efficiency η :

Equation 4:

$$EQE = \eta * IQE$$

EQE is then simply a measurement of the number of photons escaping the device per electron hole pair injected, which can be measured directly in an experiment. For the samples we grow the extraction efficiency can be estimated given the refractive index, under the assumption that all light emitted at an angle less than the critical angle to the normal will escape the device. This then gives a good measurement of the IQE.

Although it would be possible to measure the efficiency of the superlattice structures grown by EIRE by constructing LED arrays, there are many factors which can affect the efficiency of LEDs. By performing photoluminescence measurements on unmounted samples, using an external laser as the energy source, it is possible to isolate the effect of different superlattice structures on efficiency. By measuring the intensity of the laser and carefully accounting for the energy lost prior to being absorbed by the sample, it is possible to calculate the number of electron hole pairs produced by the laser. Each photon

absorbed by the sample can only produce one electron-hole pair, with the rest dissipated as heat.

Therefore the rate of pair creation scales as:

$$\text{Equation 5: } \frac{dN_{pairs}}{dt} = \frac{P_{in}}{E_{photon}} = \frac{P_{in}}{\frac{hc}{\lambda_{in}}} = \frac{P_{in} * \lambda_{in}}{hc}$$

The number of photons out is simply

$$\text{Equation 6: } N_{photons} = \frac{P_{out}}{E_{photon}} = \frac{P_{out}}{\frac{hc}{\lambda_{out}}} = \frac{P_{out} * \lambda_{out}}{hc}$$

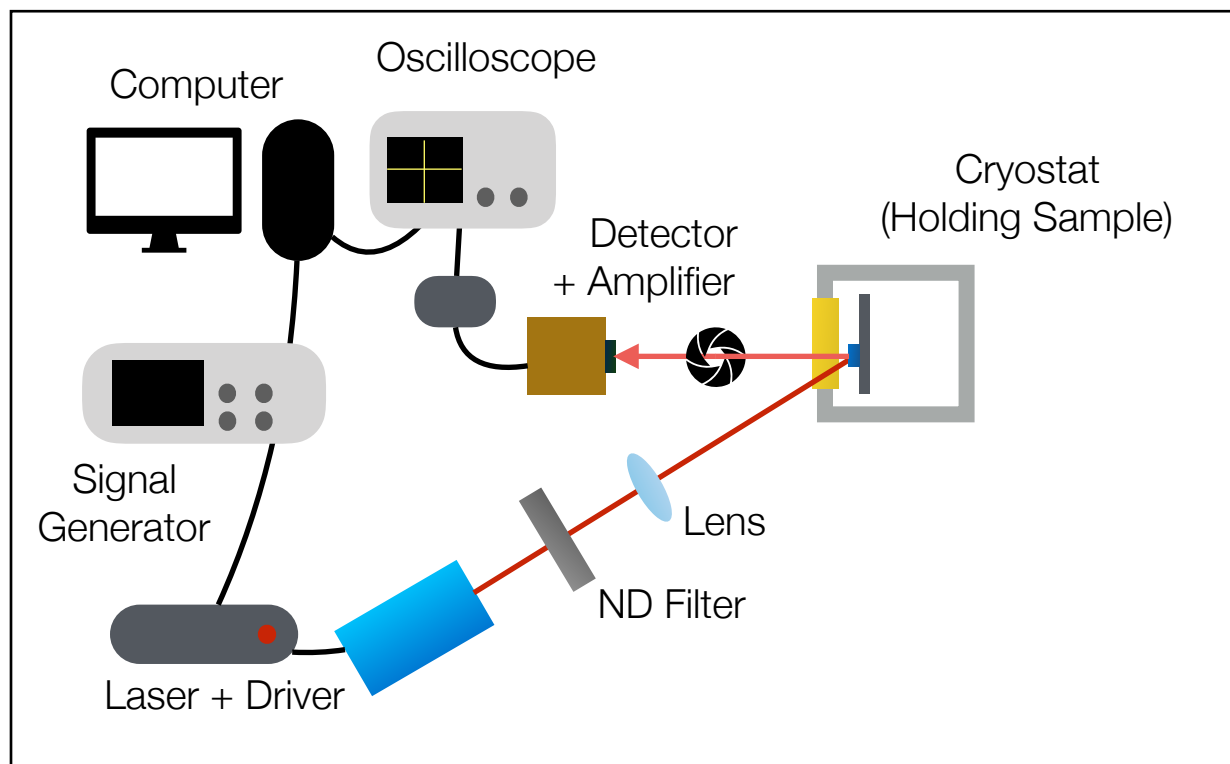
Because EQE is $N_{photons}/N_{pairs}$ this simplifies to

$$\text{Equation 7: } EQE = \frac{P_{out} * \lambda_{out}}{P_{in} * \lambda_{in}}$$

Because the wavelength of the pump laser and the superlattice emission are fixed, an EQE measurement then comes down to measuring the power output by a sample relative to the power input. However, the behavior of the device depends on the density of the electron hole pairs in the superlattice, not simply the total number. Therefore it is important to characterize the spot size of the laser to get the total intensity, and because the thickness of the superlattice is known for each sample, it is then possible to translate the intensity measurement into a pair generation rate. Using lifetime information from the ultrafast measurements it is then possible to calculate the carrier density for a given power, which allows the comparison of radiative to non-radiative recombination modes at different carrier densities.

Experiment:

The experimental setup is relatively simple, although a great deal of work was done in quantifying the amount of light actually being absorbed by the sample, as well as the spot size of the laser.

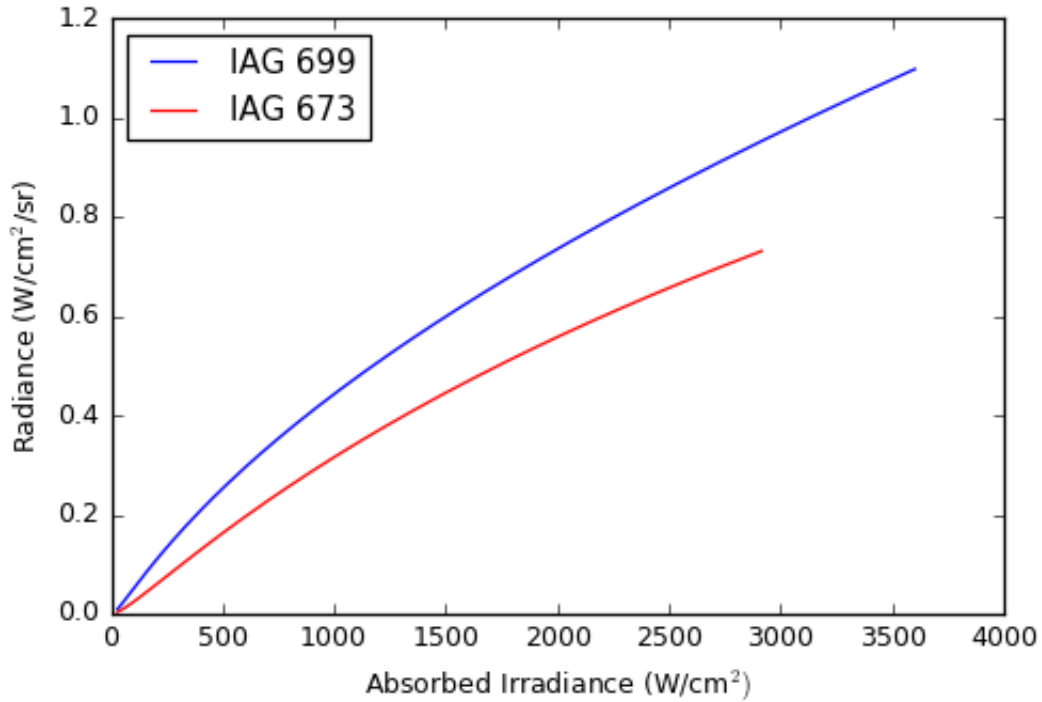


A cryostat holds the sample on a cold finger which is kept at 77K. The sample is placed so that the maximum amount of emitted light reaches the detector when illuminated by the laser. Both the laser driver and detector are connected to a computer, which allows largely automatic data acquisition. The laser is modulated across a range of intensities with a pulse repetition rate of 20 Hz and a duty cycle of 1% using a computer-controlled signal generator. The pulse waveform is necessary so as not to overheat the sample during the measurement. The beam passes through a series of steering mirrors (not pictured) and through an optional ND filter, then focused onto the sample using a fixed lens. The distance from the lens to the sample is adjusted using one axis of a 3-axis micrometer on which the cryostat is mounted. This allows an adjustment of the spot size without changing the total intensity of the laser, which allows the use of a less sensitive detection setup. An iris is placed in between the sample and the detector in order

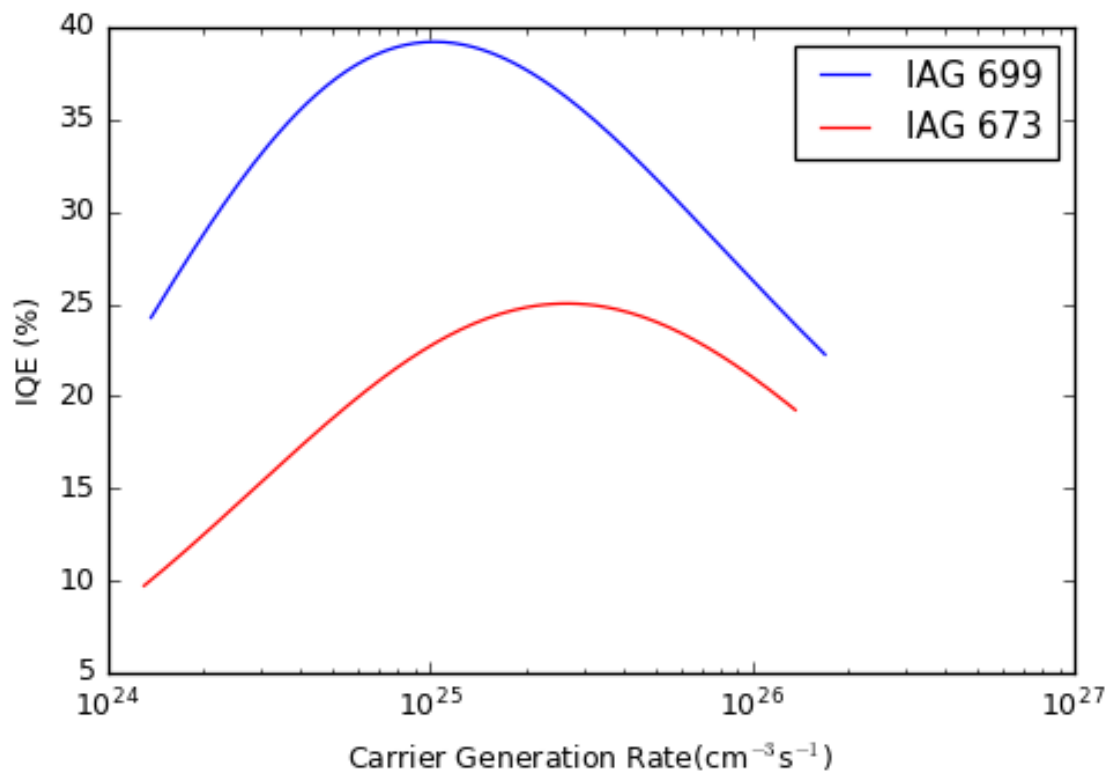
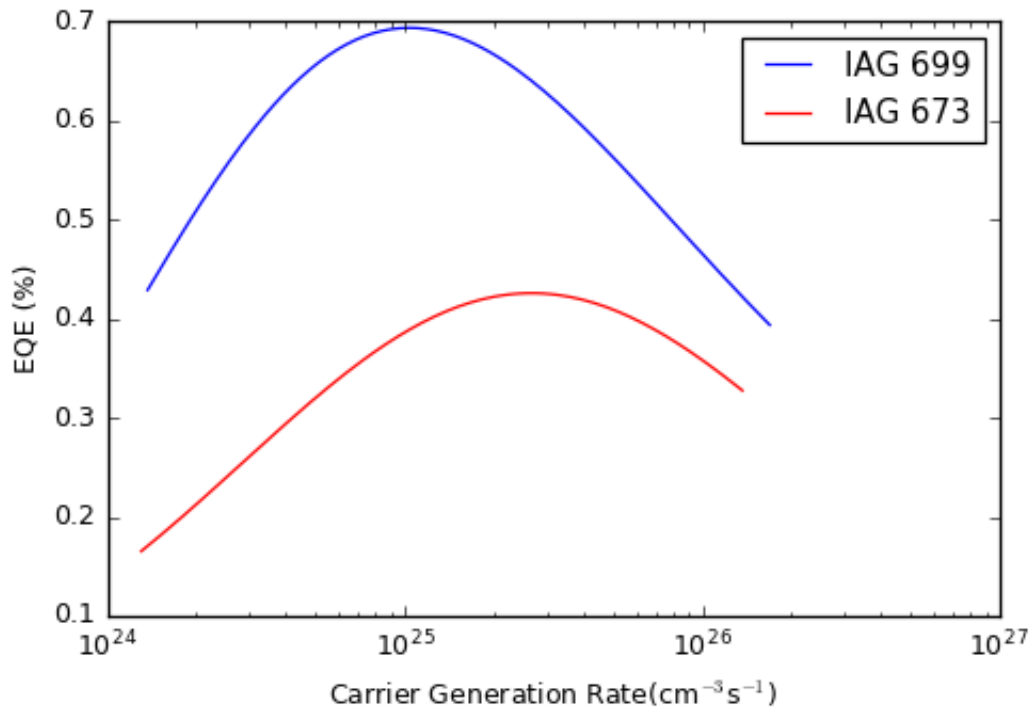
to prevent stray reflections from interfering with the measurement. The detector measures the light emitted from the sample while the laser is in operation, and is connected to an oscilloscope which is connected to a computer. The oscilloscope is necessary to capture the waveform output from the detector, allowing manipulation of the waveform on the computer, which greatly simplifies data analysis. In particular, the laser bandwidth is small enough that it takes a measurable amount of time to rise to full intensity once the modulation pulse starts and to fall to zero intensity once the pulse stops. This time delay is consistent between measurements, however, so the analysis program on the computer discards the data while the laser is rising to full intensity and falling to zero. Once the data for a full run is collected the analysis program calculates the total power emission from the front face of the sample based on the detector signal. This is calculated by converting the detector signal into power received by the detector using a responsivity value calculated from CWPL measurements. The total light emission from the front of the sample can then be calculated by assuming Lambertian emission. This gives the power output from the device, and the energy deposited in the sample is known by measuring the laser with a power meter placed where the sample would be in a normal measurement, for the case where the ND filter is or is not present. Subtracting absorption from the cryostat window and reflection from the surface of the sample then gives a deposited power value, which allows the calculation of EQE as explained in the theory section. All the preceding calculations are done automatically, so the only manual steps required are placement of the samples in the cryostat, position adjustment of samples, spot size measurement and placement and removal of the neutral density filter. For each sample in a growth series data is taken with and without the ND filter in place and at three spot sizes which allows the laser intensity to be varied over a wider range than it could be otherwise. Each run is then combined to improve the estimate of the EQE and IQE values at each intensity.

Results:

A plot of the raw data for two representative samples, IAG 699 and IAG 673, is shown below.



As can be seen above the radiance from IAG 699 and IAG 673 are approximately linear with the absorbed irradiance, but the slope decreases as the laser intensity increases. This is to be expected, as independent of other effects Auger recombination should increase at higher carrier densities, and therefore higher irradiance values. However, it is difficult to make quantitative predictions about what is happening inside the structures with the data in this format. It is more convenient to have values of EQE and IQE versus carrier creation rate, and thankfully the data can be easily changed into this format. Using Equation 7 gives EQE as a function of absorbed irradiance and radiance, and estimating the extraction efficiency from the index of refraction gives IQE values via Equation 4. Using Equation 5, it is then possible to change absorbed irradiance into carrier generation rate, which is the desired format. Thankfully, this computation is automated in the data analysis software. Plots of EQE and IQE versus carrier generation rate are shown on the following page.



Discussion:

The IQE values for each sample start relatively low, due to the dominance of SRH recombination, and increase linearly, as is expected from the form of Equation 3. The slope then decreases until it reaches a maximum and then becomes negative, which occurs when Auger recombination starts to dominate the denominator in Equation 3. In regards to the specific samples, the IQE value for IAG699 tops out at nearly 40%, which is quite good for a device operating in the Mid-IR, and IAG 673 reaches nearly 25%, which is also high, albeit inferior to IAG699. Also, the IQE values for IAG 699 were higher than that of IAG 673 at lower carrier injection rates, which suggests the SRH lifetime is longer, assuming the carrier lifetimes are similar. The curves seem to converge at higher carrier generation rates, which suggests the Auger lifetime is similar for both samples meaning that there is not a particularly large benefit in Auger recombination rate for one growth series over the other, again assuming that carrier lifetimes are similar. IAG 699 had consistently higher IQE values over the whole range, and as each sample was the best of their respective growth runs, this suggests that the material system used for IAG 699 has more potential than IAG 673. Also of importance is the data collected for the other members of IAG699 and IAG673's growth series. Each sample in the series was grown with different superlattice parameters, so comparing the relative performance for each sample gives feedback on how differences in the superlattice structure affect performance. This information, combined with ultrafast measurements of the same samples, will be useful in deciding which superlattice structures to grow in the future in order to optimize IQE. A final note is that the EQE of the samples did not exceed 1%. This is not entirely surprising, as the index of refraction of samples at the emission frequency is between 3 and 4, resulting in extremely strong total internal reflection. This suggests that methods currently being explored at IATL to improve the extraction efficiency in these devices are well-placed. This methodology will continue to be used to characterize samples grown for the EIRE project, as it complements existing techniques for characterization. The relatively high IQE of these samples suggests that superlattices are a promising material for emission in the mid-IR, and that future development of these materials is warranted.

Image credits:

Figures 4,5 and 6 were taken from a presentation given by Cassandra Bogh et al.